

Microscopic Barrier Mechanism of Ion Transport through Liquid–Liquid Interface

Nobuaki Kikkawa,[†] Lingjian Wang,[†] and Akihiro Morita^{*,†,‡}

[†]Department of Chemistry, Graduate School of Science, Tohoku University, Sendai 980-8578, Japan

[‡]Elements Strategy Initiative for Catalysts and Batteries (ESICB), Kyoto University, Kyoto 615-8520, Japan

S Supporting Information

ABSTRACT: Microscopic mechanism of ion transport through water–oil interface was investigated with molecular dynamics simulation. The formation/breaking of a water finger during the ion passage was explicitly formulated in the free energy surface. The calculated 2D free energy surface clearly revealed a hidden barrier of ion passage accompanied by the water finger. This barrier elucidates the retarded rate of interfacial ion transfer.

Transport of ions through the interface between two immiscible electrolyte solutions (ITIES) is of ubiquitous importance in many fields of chemistry, including separation and extraction, chemical sensors, phase-transfer catalysis, membrane transport, etc.^{1–3} Although the transport phenomena have been extensively treated in a number of disciplines, the understanding of the microscopic mechanism and kinetics of the interfacial transfer is still far from complete. The uncertainty in measuring the ion transfer kinetics is illustrated with the history of the reported standard rate constants of $N(C_2H_5)_4^+$ (denoted with TEA⁺) passing through the water/1,2-dichloroethane or nitrobenzene interface.⁴ The apparent standard rate constant of the interfacial ion transfer k_0 had been increasing along with the progress of measuring technologies until quite recently from 10^{-3} – 10^2 cm/s.^{4–6} Such apparent variation is largely due to the difficulties in selectively observing the interfacial transfer because the phenomenological transfer rates are affected by a number of kinetic factors other than the purely interfacial transfer. It is noteworthy that the use of nano-ITIES has greatly facilitated our understanding of the interfacial kinetics, and the micropipette apparatus may involve some artifacts on the transport.^{4,7}

The interfacial transfer kinetics were also discussed in some theories proposed to date. Those theories have dealt with various aspects of microscopic interfacial properties, such as local diffusion,^{8,9} activation barrier,^{10,11} desolvation,¹² and protrusion or structural fluctuation.^{13,14} To examine these various aspects, reliable information on the microscopic ITIES structure is of crucial importance. However, detailed information on the liquid–liquid interfaces is mainly scarce because available experimental probe techniques with sufficient sensitivity and selectivity are quite limited. The dynamic fluctuation of the interfaces is much harder to observe than the thermally averaged structure of the interfaces by experimental means. Lack of reliable information on the interfacial structure,

including the dynamical aspects, is a main obstacle toward establishing a unified theory of interfacial transfer.

To overcome those difficulties, molecular dynamics (MD) simulation is a powerful method. For example, the characteristic structural fluctuation associated with the ion transfer, called a “water finger”, was first discovered by Benjamin with his MD simulation.¹⁵ However, the application of MD simulation has a severe limitation in both spatial and temporal scales. The diffusion dynamics of ion passage is hard to trace within the time scale of MD simulation. Therefore, we describe this process in terms of the relevant free energy surface. The landscape of the free energy surface and the diffusive properties on the surface could offer invaluable insight into the mechanism of the ion transfer.

Because the free energy surface is drawn with selected coordinate(s), the choice of the relevant coordinate is crucial. A natural choice is the coordinate of the transferring ion normal to the liquid–liquid interface, namely z , where the origin $z = 0$ is set at the Gibbs dividing surface of water so that $z < 0$ means that the ion is in water phase and $z > 0$ means it is in the oil phase. This coordinate z naturally connects two asymptotic regions over the ion passage, and has been used as a reaction coordinate.^{16–23} The calculated free energy profiles as such reported almost no barrier during the passage of small inorganic ions. These MD results appear inconsistent with the previous assumption of an activation process, which aimed at explaining the rate constant ($k_0 = 0.1$ – 1.0 cm/s) that was smaller than the diffusion-limited one, 100 cm/s.¹³ It is rather conceivable that the conventional free energy surface on the z coordinate does not properly describe the activation barrier.

In performing the MD simulation of ion transport, we often encounter hysteresis of structure associated with the water finger formation/break,^{18,19,22} which implies that there exist two stable states of interface structure at the same position of z . To distinguish the two states and possible transition between the states, another coordinate relevant to water finger is indispensable. Some previous studies of ion transports tried to consider the water finger.^{13,14,24–26} For example, Schweighofer and Benjamin tried to describe the change of the water finger by using solvation energies,²⁴ and Darvas et al. found a barrier via analyzing the interfacial fluctuation.²⁵ Despite these efforts, a proper coordinate has not yet been established that is well-defined and amenable to the MD simulation. The present paper defines a proper coordinate of water finger, which allows for

Received: May 3, 2015

Published: June 9, 2015



comprehensive 2D free energy surface against the ion position and the water finger by using MD simulation.

The coordinate relevant to the water finger should satisfy several conditions. It should pinpoint the water finger formation and break and be defined from instantaneous molecular configuration as well as being continuous and differentiable. To satisfy those requirements, we employed the graph theory, where the ion and water molecules are regarded as vertices. The connectivity between vertices depends on an assumed threshold distance: if the distance between two vertices is smaller/larger than a given threshold, then the two vertices are judged as connected/disconnected. Thus, the water-finger coordinate, w , is naturally defined as the minimum threshold to make the ion and the bulk water reachable, which is illustrated in Figure 1. The details of the definition are given in Supporting Information.

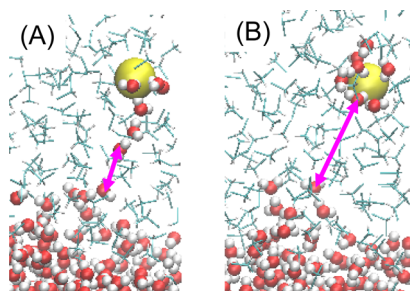


Figure 1. Water finger coordinates (distance of pink arrows) in two cases of water finger: (A) formed and (B) broken. Yellow balls stand for Cl^- ions, red and white balls stand for oxygen atoms and hydrogen atoms of water, respectively, and blue and white sticks stand for DCM molecules.

We calculated the 2D free energy surface of ion transport with z and w . The MD simulation was performed for Cl^- transport through water and dichloromethane (DCM) interface. We employed polarizable molecular models^{18,27} to improve accuracy in the free energy calculations because nonpolarizable models tend to excessively overestimate the free energy of interphase transfer. We performed the free energy calculation with replica exchange umbrella sampling²⁸ (REUS). The REUS method can facilitate the sampling of connecting/disconnecting water fingers. Detailed protocols of the MD simulation are also given in Supporting Information.

Figure 2 shows the calculated 2D free energy surface, $G^{(2)}(z, w)$, 1D surface, $G^{(1)}(z)$, and the representative snapshots of some points in the 2D surface. Note that the 1D surface is derived from the former by

$$G^{(1)}(z) = -k_B T \ln \int dw \exp[-G^{(2)}(z, w)/k_B T] \quad (1)$$

where k_B and T are the Boltzmann constant and temperature, respectively. The 1D surface, $G^{(1)}(z)$, exhibits no barrier along the z coordinate, consistent with previous MD studies.^{17–19,22,25} The free energy difference between the asymptotic regions is 16 kcal/mol, which agrees fairly well with the value of previous MD simulation, 14 ± 2 kcal/mol.¹⁸ In contrast, the 2D surface, $G^{(2)}(z, w)$, reveals two valleys, denoted A and B. Valley A, characterized by a smaller w , indicates a path with the water finger formation, whereas B indicates a path with a broken water finger. The presence of the two states can explain the hysteresis of ion transport associated with water finger formation/breaking and also implies that a

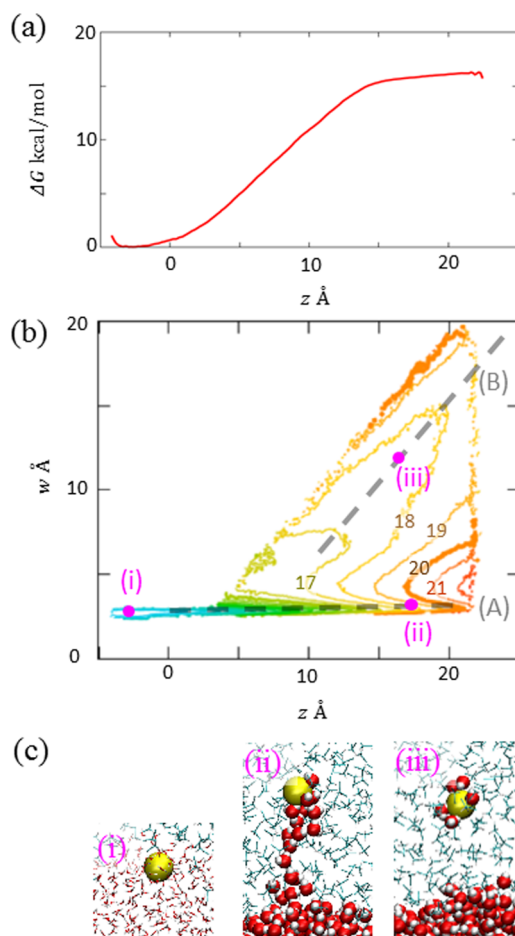


Figure 2. (a) 1D free energy surface $G^{(1)}(z)$ with the origin $G = 0$ set at the minimum near the interface. (b) 2D surface $G^{(2)}(z, w)$, where the contour values are shown with 1 kcal/mol interval. Two paths (A and B) are illustrated in gray dashed lines, and three representative locations on the paths (i–iii) are indicated. (c) Typical snapshots at i–iii, where the symbols are same as those of Figure 1. (Only snapshot I uses the stick form for water molecules to make the embedded Cl^- visible).

transition between the states is involved along the ion transport.

Figure 3 displays the distribution of hydrated water number immediately after the break of the water finger. The hydration number is well-defined from the connectivity of hydrogen bonds in the present work, and the present MD simulation allows reliable sampling of hydration number distribution through the intensive sampling of the transition events over the

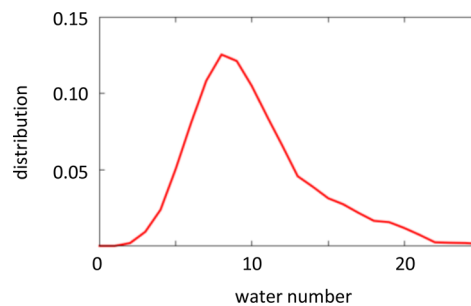


Figure 3. Distribution of hydrated water number of Cl^- in the oil phase just after the break of water finger at $w = 5\text{--}6$ Å.

water finger formation and break. First, we find that the nascent clusters have 10.0 water molecules on average, and larger clusters are also frequently generated. In contrast, few ions have 0–2 solvating waters just after the break, which is consistent with previous MD work.^{29,30} These typical solvation numbers of the nascent clusters are significantly larger than those estimated experimentally in the stable bulk phase of 1,2-dichloroethane, 2.7.³¹ It implies subsequent dynamics of water evaporation during the ion passage. Further study on the role of evaporation is now in progress.

The above calculations of Figures 2 and 3 assumed a situation free from external potential and influence of other ions, though the actual ion transport takes place with an assist of external potential and electric double layer. To take into account these influences, the free energy surface was calculated by imposing a certain external field, 0.1 or 0.2 V/nm, and the results are shown in Figure 4. The 1D surfaces in Figure 4a

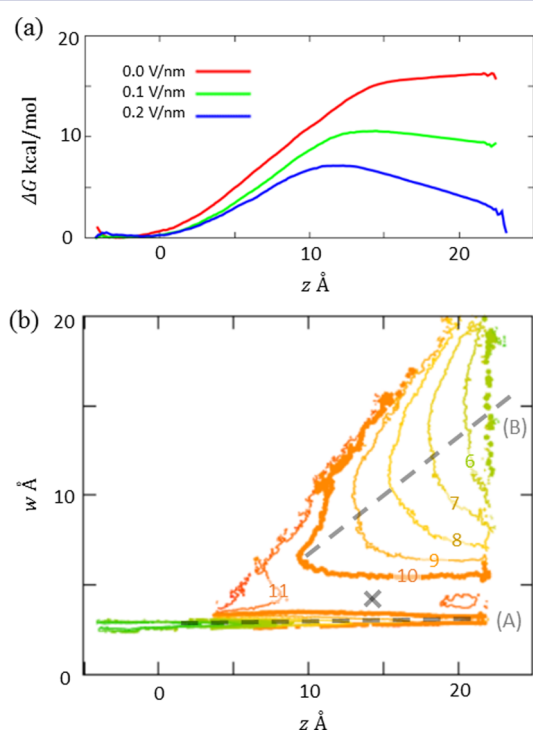


Figure 4. (a) 1D surface $G^{(1)}(z)$ with external fields 0.0–0.2 V/nm. (b) 2D surface $G^{(2)}(z, w)$ with the field of 0.2 V/nm; the contour values are shown with 1 kcal/mol intervals. Two valleys (A and B, dashed lines) and the saddle point (cross) are shown in gray.

indicate that the external field facilitates the ion transport from water to oil phase by lowering the free energy barrier. At 0.2 V/nm, the barrier is estimated to be 7.1 kcal/mol in the 1D surface. Figure 4b displays the 2D free energy surface under the field. The panel shows a saddle point at ($z = 14$ Å, $w = 4$ Å) that connects the two valleys A, with water finger, and B, without water finger. The ion near the water phase ($z < 10$ Å) is stable on valley A, whereas the asymptotic region in the oil phase is stable on the B side. Therefore, the ion has to pass the ridge between the two valleys during the interfacial transfer. We note that the barrier height at the saddle point is 11 kcal/mol, which is significantly larger than that at the barrier in the 1D surface mentioned above. The excessive barrier height (by 4 kcal/mol) manifests itself in the 2D surface because the transition over the barrier occurs along the w coordinate; thus,

it is characterized by the change of water finger structure. As a rough estimate, the excessive free energy barrier of $\Delta G = 4$ kcal/mol should result in the reduction of reaction rate by $\exp[-\Delta G/(k_B T)] \approx 1.2 \times 10^{-3}$ at room temperature. This ratio could account for the observed rate (~ 0.1 cm/s) in comparison to the diffusion-limited one ($\sim 10^2$ cm/s).¹³

In the present paper, we formulated a proper coordinate of water finger formation during the ion passage and thereby performed the MD computation of 2D free energy surface of Cl^- transfer over water/DCM interface. The MD simulation allows us to explicitly take into account the water finger coordinate and to examine the microscopic mechanism of ion transport with realistic molecular models. The MD results revealed a hidden barrier of ion passage, which is accompanied by the formation and breaking of the water finger. This finding could elucidate the observed rate of ion transfer that is different from the diffusion-limited one. We are now further investigating the transfer mechanism in details, involving the role of hydration and electric double layer using MD simulation.

■ ASSOCIATED CONTENT

📄 Supporting Information

The Supporting Information is available free of charge on the ACS Publications website at DOI: 10.1021/jacs.5b04375.

■ AUTHOR INFORMATION

✉ Corresponding Author

*morita@m.tohoku.ac.jp

Notes

The authors declare no competing financial interest.

■ ACKNOWLEDGMENTS

We thank Prof. S. Amemiya for helpful discussion. This work was supported by the Grants-in-Aid for Scientific Research (nos. 25104003 and 26288003), JSPS and MEXT, Japan.

■ REFERENCES

- (1) *Faraday Discuss.* **2005**, *129*, 1–370.
- (2) Girault, H. H. In *Electroanalytical Chemistry: A Series of Advances*; Bard, A. J., Zoski, C. G., Series Eds.; CRC Press: Boca Raton, FL, 2010; Vol. 23, pp 1–104.
- (3) Dryfe, R. A. W. *Adv. Chem. Phys.* **2009**, *43*, 153–215.
- (4) Samec, Z. *Electrochim. Acta* **2012**, *84*, 21–28.
- (5) Li, Q.; Xie, S.; Liang, Z.; Meng, X.; Liu, S.; Girault, H. H.; Shao, Y. *Angew. Chem., Int. Ed.* **2009**, *48*, 8010–8013.
- (6) Gavach, C.; D'Epenoux, B.; Henry, F. *J. Electroanal. Chem.* **1975**, *64*, 107–115.
- (7) Silver, B. R.; Holub, K.; Marecek, V. *J. Electroanal. Chem.* **2014**, *731*, 107–111.
- (8) Shao, Y.; Girault, H. H. *J. Electroanal. Chem.* **1991**, *282*, 59–72.
- (9) Kakiuchi, T. *J. Electroanal. Chem.* **1992**, *322*, 55–61.
- (10) D'Epenoux, B.; Seta, P.; Amblard, G.; Gavach, C. *J. Electroanal. Chem.* **1979**, *99*, 77–84.
- (11) Schmickler, W. *J. Electroanal. Chem.* **1997**, *426*, 5–9.
- (12) Aoki, K. *Electrochim. Acta* **1996**, *41*, 2321–2327.
- (13) Marcus, R. A. *J. Chem. Phys.* **2000**, *113*, 1618.
- (14) Kornyshev, A. A.; Kuznetsov, A. M.; Urbakh, M. *J. Chem. Phys.* **2002**, *117*, 6766.
- (15) Benjamin, L. *Science* **1993**, *261*, 1558–1560.
- (16) Schweighofer, K.; Benjamin, I. *J. Phys. Chem. A* **1999**, *103*, 10274–10279.
- (17) Dang, L. X. *J. Phys. Chem. B* **1999**, *103*, 8195–8200.
- (18) Dang, L. X. *J. Phys. Chem. B* **2001**, *105*, 804–809.

- (19) dos Santos, D. J.; Gomes, J. A. *ChemPhysChem* **2002**, *3*, 946–951.
- (20) Wick, C. D.; Dang, L. X. *J. Phys. Chem. C* **2008**, *112*, 647–649.
- (21) Darvas, M.; Jorge, M.; D. S. Cordeiro, M. N.; Jedlovszky, P. *J. Phys. Chem. C* **2011**, *115*, 11140–11146.
- (22) Kikkawa, N.; Ishiyama, T.; Morita, A. *Chem. Phys. Lett.* **2012**, *534*, 19–22.
- (23) Benjamin, I. *J. Phys. Chem. B* **2013**, *117*, 4325–4331.
- (24) Schweighofer, K. J.; Benjamin, I. *J. Phys. Chem.* **1995**, *99*, 9974–9985.
- (25) Darvas, M.; Jorge, M.; Cordeiro, M. N.; Kantorovich, S. S.; Sega, M.; Jedlovszky, P. *J. Phys. Chem. B* **2013**, *117*, 16148–16156.
- (26) Daikhin, L. I.; Kornyshev, A. A.; Kuznetsov, A. M.; Urbakh, M. *Chem. Phys.* **2005**, *319*, 253–260.
- (27) Caldwell, J. W.; Kollman, P. A. *J. Phys. Chem.* **1995**, *99*, 6208–6219.
- (28) Sugita, Y.; Kitao, A.; Okamoto, Y. *J. Chem. Phys.* **2000**, *113*, 6042–6051.
- (29) Benjamin, I. *J. Phys. Chem. B* **2008**, *112*, 15801–15806.
- (30) Rose, D.; Benjamin, I. *J. Phys. Chem. B* **2009**, *113*, 9296–9303.
- (31) Kusakabe, S.; Arai, M. *Bull. Chem. Soc. Jpn.* **1996**, *69*, 581–588.